SLA 3-D Printed Arrays of Miniaturized, Internally Fed, Polymer Electrospray Emitters

Luis Fernando Velásquez-García, *Senior Member, IEEE*

***Abstract*— This paper reports the design, fabrication, and characterization of arrays of miniaturized, internally fed, polymer electrospray emitters fabricated with stereolithography. The freeform additive manufacturing process used to make the devices has associated two orders of magnitude reduction in the fabrication cost per device and fabrication time (from thousands of dollars to tens of dollars, and from months to hours, respectively) and a two orders of magnitude reduction in the cost of the manufacturing infrastructure (from millions of dollars to tens of thousands of dollars) compared with a silicon MEMS multiplexed electrospray source. The 3-D printed devices include features not easily attainable with other microfabrication methods, e.g., tapered channels and threaded holes. Through the optimization of the fabrication process 10-mm tall, isolated, straight, solid columns with diameter as small as 300 μm, and 12-mm long, straight tubes with inner diameter as small as 400 μm and wall thickness as small as 150 μm were demonstrated. Arrays with as many as 236 internally fed electrospray emitters (236 emitters in 1 cm^2) were made, i.e., a twofold increase in emitter density and a sixfold increase in array size compared with the best reported values from multiplexed, internally fed, electrospray sources made of polymer. The characterization of devices with a different array size suggests a uniform emitter operation. [2015-0129]**

***Index Terms*— Additive manufacturing of MEMS, electrospray, multiplexed liquid ionizers, stereolithography.**

I. Introduction

ELECTROSPRAY, i.e., the ionization of liquids using high electric fields [1], is a physical phenomenon that produces from a meniscus a stream of micro/nanoparticles that, depending on the properties of the liquid and the process conditions, can be droplets [2], ions [3], or fibers [4]. The low variation in size and specific charge of the emitted particles makes the use of electrospray attractive in applications such as combustors [5], maskless micro and nanomanufacturing [6], and nanosatellite propulsion [7]. However, the current emitted and the flow rate of an electrospray emitter is very low (typically <10 μA and <10 μl/min, respectively), limiting the applicability of single-emitter electrospray sources to a few practical cases, e.g., mass spectrometry of biomolecules [8].

An approach to increase the throughput of an electrospray source without affecting the size variation of the emission is implementing arrays of electrospray emitters that operate in parallel. Miniaturization of the electrospray emitters results in less power consumption and lower onset voltage; in addition, using microfabrication, monolithic arrays of miniaturized emitters with large array size and emitter density can be made. Researchers have demonstrated a variety of MEMS multiplexed electrospray sources that operate uniformly, i.e., monolithic arrays of microfabricated electrospray emitters that operate in parallel where each emitter approximately contributes the same amount to the total output of the source [5], [9]–[15]. These devices work satisfactorily, although they present a number of issues:

- The device architecture is usually a compromise between what should be made based on the modeling and what can be made given the planar nature and thickness limitation of traditional microfabrication, often sacrificing device performance. Fabrication approaches that can monolithically integrate microscaled and mesoscaled features at ease and that enable great freedom in the morphology and structure of the system should yield better devices. For example, in some cases it would be advantageous to provide taper to the emitters [16] to facilitate the deposition of directional coatings on their outer and/or inner surfaces. Moreover, it would be beneficial to include interfacing structures, e.g., threaded holes, monolithically incorporated into the device to facilitate its integration to an apparatus while reducing the overall footprint.
- In these devices, a change in any of the in-plane features of the design typically requires the design and fabrication of one or more new lithography masks. Therefore, the iteration of the design often incurs in substantial costs and time delays.
- In some cases, the microfabricated electrospray sources include complex hydraulic networks that require advanced microfabrication techniques such as wafer bonding and multi-nested etch masks [17], which increases the production cost of the devices and could also decrease their fabrication yield.
- In many cases, the electrospray arrays are made of single-crystal silicon, which is an expensive material. In addition, applications not compatible with the properties of silicon, e.g., opaqueness to visible light, cannot be satisfied.
- The manufacture of MEMS multiplexed electrospray arrays is fairly expensive ($\sim$a few thousand US dollars per device) because they are made in a multi-million semiconductor-grade cleanroom with advanced tools that

Manuscript received May 10, 2015; revised July 13, 2015; accepted August 30, 2015. Date of publication September 14, 2015; date of current version November 25, 2015. Subject Editor A. Luque.

The author is with the Microsystems Technology Laboratories, Massachusetts Institute of Technology, Cambridge, MA 02139 USA (e-mail: velasquez@alum.mit.edu).

Color versions of one or more of the figures in this paper are available online at http://ieeexplore.ieee.org.

Digital Object Identifier 10.1109/JMEMS.2015.2475696

are operated by highly trained staff, restricting the application of multiplexed electrospray ionizers to high-end applications and research.

Stereolithography (SLA) is a kind of additive manufacturing, which are a group of layer-by-layer fabrication methods that use a computer file to generate solid objects [18]. Additive manufacturing started as a visualization tool of passive, mesoscaled parts; however, given the recent improvements in the resolution capabilities and cost of commercial 3-D printers, additive manufacturing has become a fabrication technology that could address the complexity, three-dimensionality, and material processing compatibility of certain microsystems, including fully assembled mechanisms [19]. Examples of reported 3-D printed MEMS include hybrid couplers and RF switches for millimeter-wave systems [20], gyroscopes [21], and 3-D antennas [22].

This work explores the use of cost-competitive, commercial, precision SLA 3-D printers to manufacture multiplexed, internally fed, polymer electrospray sources to address the aforementioned issues. The design of the 3-D printed electrospray sources is described in Section II, while the fabrication of the devices and the exploration of the resolution capabilities of the fabrication technique are documented in Section III. The experimental characterization of the liquid ionizers is described in Section IV, and a discussion of the results is provided in Section V.

II. Device Design

Perspective and front views of a computer-aided design (CAD) file that describes a 3-D printed, multiplexed electrospray source are shown in Figure 1. The device is a planar array of miniaturized, internally fed electrospray emitters. The main frame is a solid block 3 mm thick with a square base 24 mm wide. The frame includes 4 evenly spaced 4-40 threaded through-holes that can be used to clamp the device to a chuck with a liquid feedthrough. The design of the device includes the following features:

- Each emitter is internally fed by a slightly tapered converging channel with the intention to decouple the pressure required to fill-in the emitter and the pressure needed to set a flow rate through the emitter. For a circular pipe, the maximum pressure before breaking up a meniscus, P_B, is given by

$$P_B = \frac{4\gamma}{\emptyset_{ID}} \tag{1}$$

  where γ is the surface tension of the liquid and $\emptyset_{ID}$ is the inner diameter of the pipe. In a straight pipe, the fill-in pressure is the same pressure that would cause dripping at the other end of the channel. In a tapered pipe the two pressures are decoupled, and in a converging tapered pipe the fill-in pressure is lower than the dripping pressure.
- Each emitter inlet has a smooth transition that covers the space between adjacent emitters to reduce the stagnation zones in the flow field.
- Between each threaded hole and the array of emitters, there is a curved vertical wall that blocks direct contact between the hole and liquid dripped by the emitters. The threaded holes can be used to integrate a proximal extractor grid to the emitter array (see Section IV). Therefore, in such case, the curved vertical walls improve the resilience of the device against electrical breakdown due to liquid flooding.
- Each emitter tip is fed by a long and narrow channel that acts as a large hydraulic resistor because uniform electrospray array operation requires each emitter to be regulated by a fluidic ballast that controls the emitter flow rate [11], [23]. In addition, monolithic integration of the hydraulic ballast within the footprint of the emitter facilitates achieving high emitter density.
- Similar to most electrospray sources reported in the literature, the shape of the emitters helps concentrate the electric field on the liquid menisci, lowering the onset voltage. In general, the exterior of an electrospray emitter is a whisker-like/sharp conical equipotential surface surrounded by air or vacuum that generates higher normal electric fields on the tip of the emitter (i.e., where the liquid is ionized) compared to those set by a flat electrode. In our case, the column of liquid acts as an electric field enhancer, and emitters made of a thin polymer wall surrounding the liquid, instead of a continuous polymer media, should help lower the bias voltage required to turn-on the emitters. Researchers have shown that a flat metallic plate and a non-wetting flat dielectric plate with a non-protruding hole can sustain electrospray [24], [25]; however, lower bias voltage is required to activate the

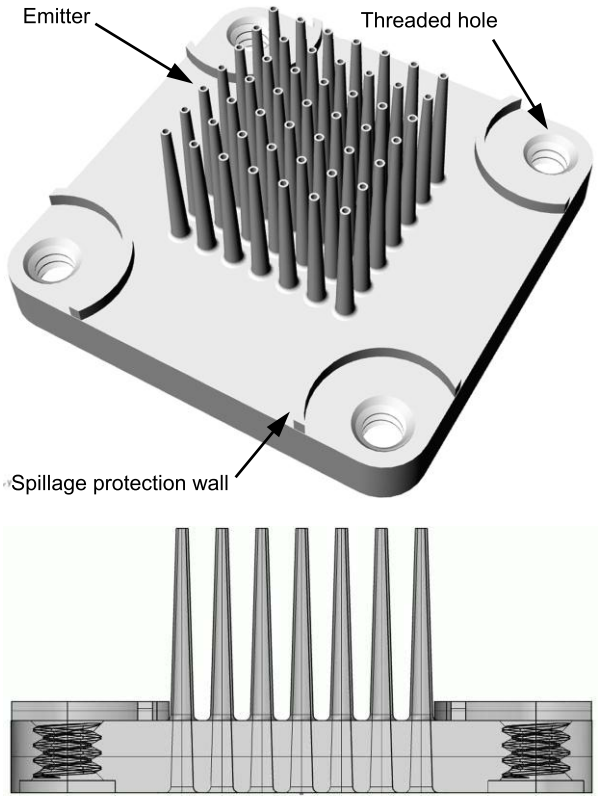

Fig. 1. Rendered perspective view (top) and X-ray front view (bottom) of 3-D printed planar array of 49 internally fed electrospray emitters. Device features include tapered internal channels, threaded holes, and spill protection features.

emission in the latter case because of the dielectric nature of the media where the channels are embedded.

- The emitters have the smallest inner diameter possible given the pixelation of the 3-D printer and the expected large utilization of the array. On the one hand, having a small emitter tip results in lower onset voltage because the electric field required to trigger electrospray emission corresponds to having the electrostatic pressure equal to the surface tension pulling

$$\frac{1}{2}\varepsilon_o E_n^2 \sim \frac{4\gamma}{\emptyset_{ID}} \tag{2}$$

where ε_o is the permittivity of free-space, $\emptyset_{ID}$ is the inner diameter of the emitter, and E_n is the normal surface electric field [26]

$$E_n \sim \frac{V}{\emptyset_{ID}} \tag{3}$$

where V is the bias voltage. On the other hand, the dimensions of the emitter spouts should have low spread across the array for them to work uniformly in parallel using the same bias voltage. Therefore, it is proposed to make the minimum feature size (MFS) of the emitters, e.g., emitter wall and emitter inner diameter, about an order of magnitude larger than the pixelation of the 3-D printer. The 3-D printer used in this work has a measured XY pixelation (e.g., in-plane size of the pixels) of 30 μm, which is about the resolution of standard precision machining ($\sim$25 μm), resulting in a device MFS on the order of 300 μm or larger. There are commercial stereolithographic 3-D printers with submicron XY pixelation, e.g., the Nanoscribe [27], but their cost is about fifty times larger than the cost of the 3-D printer used in this work ($\sim$US $10K).
- A low-cost, proximal extractor electrode is integrated to the device to reduce the onset voltage as well as to improve the beam transmission to the collector electrode. Each device uses as extractor electrode a laser-cut 250 μm-thick stainless steel flat plate with apertures that match the array of emitters. The extractor electrode is integrated to the array of electrospray emitters using dielectric screws and posts (see Section IV).
- The 3-D printed devices reported in this work emit droplets when ionizing a solution of Rhodamine B, bovine serum albumin and StabilGuard Choice microarray stabilizer (see Section IV). However, depending on the working liquid and the process conditions, an electrospray source can emit ions, droplets, or fibers [2]–[4]. For example, we recently reported an externally fed array of electrospray emitters that, depending on the concentration of the PEO polymer melt, produces droplets (low w/v PEO concentration) or nanofibers [28]. The kind of particles generated by the electrospray source and the working liquid are dictated by the application satisfied by the 3-D printed device.

III. Device Fabrication

The devices were made with a SLA 3-D printer Asiga Pico Plus 27 [29] that has a minimum Z pixelation of 1 μm (from the manufacturer) and a measured XY pixelation of 30 μm. The XY pixelation reflects the pixel size of the array of laser diodes that the tool uses to generate, layer by layer, the solid object, while the minimum Z pixelation comes from the specifications of the servo that moves the platform that supports the printed part during fabrication. The printer creates solid objects with a precision in XY of 0.5 pixels per cm ($\sim$15 μm/cm), while the servo that controls the Z pixelation has a movement resolution of 200 nm. The Asiga Pico Plus 27 is part of a new generation of cost-competitive, commercial SLA 3-D printers with a tenfold improvement in the XY pixelation compared to standard additive manufacturing printers ($\sim$250 μm), which makes possible the fabrication of microfluidics and other microsystems with adequate precision.

Stereolithography is an additive fabrication process that uses a CAD file to manufacture structures based on spatially controlled solidification of a liquid resin by photo-polymerization [30]. Stereolithography allows great freedom in the device architecture. The manufacturing process developed to make the devices has associated a two orders of magnitude reduction of the fabrication cost per device (from thousands of dollars to tens of dollars), a two orders of magnitude reduction of the manufacturing time (from months to hours), and a two orders of magnitude reduction in the cost of the infrastructure used in manufacturing the devices (from millions of dollars to tens of thousands of dollars) compared to a silicon MEMS multiplexed electrospray source.

The fabrication of the electrospray arrays uses the photosensitive polymer PlasCLEAR, made by Asiga, which is a liquid with honey-like consistency. The electrospray devices were made of a transparent polymer to facilitate flow visualization using visible light, making possible procedures such as assessing whether the fluidic network is properly filled-in. The puddle of liquid used in the printing process needs to be free of particles and of remnants from previous runs. A computer program creates the CAD file of the printed object, and a second computer program uses the CAD file to generate a series of cuts of the printed part that are transmitted to the printer. The CAD file can be sliced into 1 μm-thick cuts or thicker; we typically sliced the CAD file into 25 μm-thick cuts to have the Z pixelation similar to the XY pixelation. After the printing job is completed, the device is removed from the building platform using a spatula, and the part is thoroughly cleaned in isopropyl alcohol (IPA). It is important to remove all unexposed (liquid) polymer from the part, particularly from the internal cavities; otherwise, the unexposed liquid will be solidified when the part is cured. By trial and error it was determined that a series of cleaning procedures using an ultrasound bath while heating the IPA with a water bath gives satisfactory results. After cleaning, the device is dried using a nitrogen gun and is then exposed to UV light for 2 minutes in an inert atmosphere to strengthen the part. Finally, the devices are stored in a nitrogen box.

Even though the fabrication of the electrospray devices is greatly simplified by the use of stereolithography, a SLA 3-D printer is quite different compared to a standard printer of paper documents in the sense that significant tuning of the different parameters that control a printing job needs

to be done to successfully print a part with hundreds-of-micrometers-large features. As a matter of fact, printing the devices using the parameters provided by the vendor did not yield good results; this is not surprising because the Asiga SLA printers are designed to generate wax masters of mesoscaled, void-free jewelry with low aspect-ratio surface details, and printing these wax masters typically involves thicker cuts of the CAD file (the smaller the cuts the slower the printing process). Through a systematic exploration of the parameters that control the printing job, a recipe that satisfactorily creates the electrospray arrays with good repeatability was obtained. In particular, the speed of the building platform as it moves in and out of the photosensitive polymer puddle was substantially reduced, the waiting time between movements of the platform was considerably increased, and the exposure time was significantly augmented. However, unlike silicon MEMS multiplexed electrospray sources, the process parameters adjusted for the fabrication of an n-by-n array can be directly used to satisfactorily print devices with any other array size and/or emitter pitch provided the emitter element is not modified. Furthermore, the fabrication process does not seem to drift, e.g., over a hundred electrospray arrays were printed across a year while using the same printing recipe–even though various array sizes of the same device, diverse microfluidics and other structures, and different batches of PlasCLEAR were used. The consistency of the SLA manufacturing process is very different to, for example, the consistency of deep reactive-ion etching (DRIE) recipes, particularly in a shared microfabrication facility, which are commonly used to manufacture silicon MEMS multiplexed electrospray sources.

The capabilities of the tweaked SLA manufacturing process were investigated. Figure 2 shows a linear array of 7 isolated, straight, solid columns; the columns are 10 mm tall and the diameter varies between 300 μm and 900 μm. Based on metrology of high-resolution images, the dimensions of the printed columns are within 15 μm of the corresponding dimensions in the CAD file; from metrology of the images it was also confirmed that the difference between the diameters of adjacent columns is constant, in other words, that the values of the diameter of the array of columns uniformly spanned the 900 μm-to-300 μm range. The thinnest straight column has a diameter of 300 μm and an aspect ratio of 33. Columns of smaller diameter were printed but they curled during the post-printing processing, likely due to the interaction of the printed structures with the receding IPA wetting front during drying. The columns were straight within the IPA bath after removing the unexposed polymer, right before the drying and UV curing steps; the receding wetting front during drying possibly caused plastic deformation of the structures as they were not stiff enough to overcome the surface tension pulling. Table 1 summarizes the mechanical properties of the photosensitive polymer PlasCLEAR after printing (from the vendor)–a soft plastic. As an example, the flexural strength and flexural modulus of silicon are 1 GPa and 150 GPa, respectively [32].

Figure 3 shows an array of 9 isolated, straight, vertical walls; the walls are 10 mm tall and the thickness of the straight walls varies between 400 μm and 600 μm. Based on

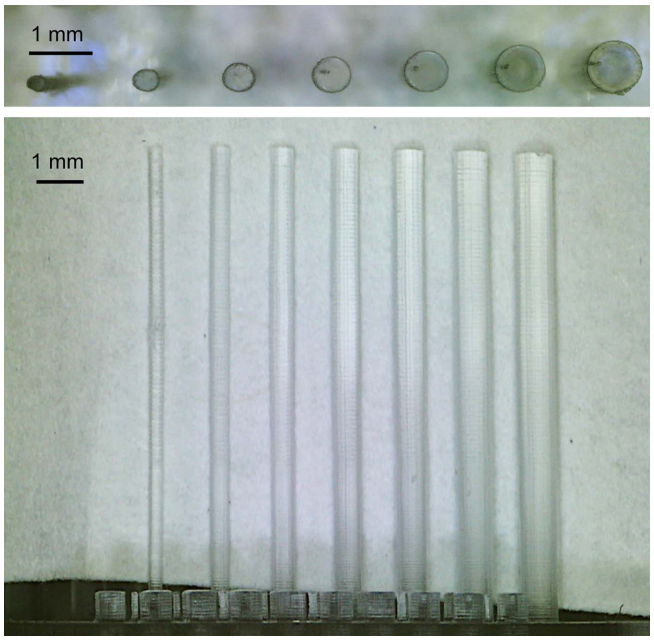

Fig. 2. A series of 10 mm tall straight, solid columns printed using stereolithography. The column diameter varies between 300 μm a 900 μm in steps of 100 μm, increasing from left to right. The writing used to label the print can be seen on the bottom of the array.

TABLE I
MECHANICAL PROPERTIES OF THE PHOTOSENSITIVE POLYMER PlasCLEAR AFTER PRINTING (FROM [31])

Property	Value
Tensile strength	52.6 MPa
Flexural strength	87.3 MPa
Flexural modulus	1915 MPa
Hardness	79 Shore D
Izod notched impact	4.91 kJ/m^2

metrology of high-resolution images of the printed objects, the dimensions of the walls are within 15 μm of the corresponding dimensions in the CAD file; from metrology of the images it was also confirmed that the difference between the thickness of adjacent walls is constant, i.e., that the values of the thickness of the series of walls uniformly spanned the 600 μm-to-400 μm range. Walls with thickness as small as 225 μm were printed but they curled during the post-printing processing. The manufacture of dense arrays of straight columns was also explored; arrays of columns with aspect ratio as large as 17, diameter as small as 179 $\pm$ 10 μm, and center-to-center column separation as small as 200 μm $\pm$ 4 μm were fabricated (Figure 4).

Through optimization of the fabrication process, devices with as many as 143 tapered electrospray emitters in 1 cm^2 were made (i.e., the arrays of emitters are hexagonally packed with 888 $\pm$ 7 μm emitter pitch); in these devices each emitter spout is fed by a 12 mm long tapered internal channel with 400 $\pm$ 15 μm diameter at the emitter spout and 498 $\pm$ 10 μm diameter at the emitter inlet (Figure 5). In addition, devices with as many as 236 straight electrospray emitters in 1 cm^2

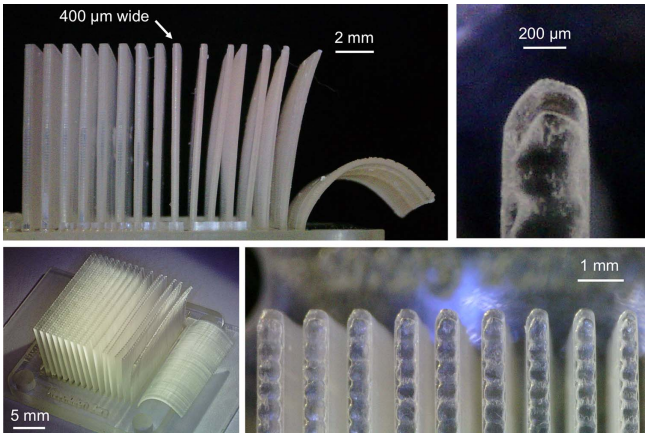

Fig. 3. A series of 10 mm tall straight, vertical walls printed with stereolithography. The wall thickness of the straight structures varies between 400 μm and 600 μm in steps of 25 μm, decreasing from left to right.

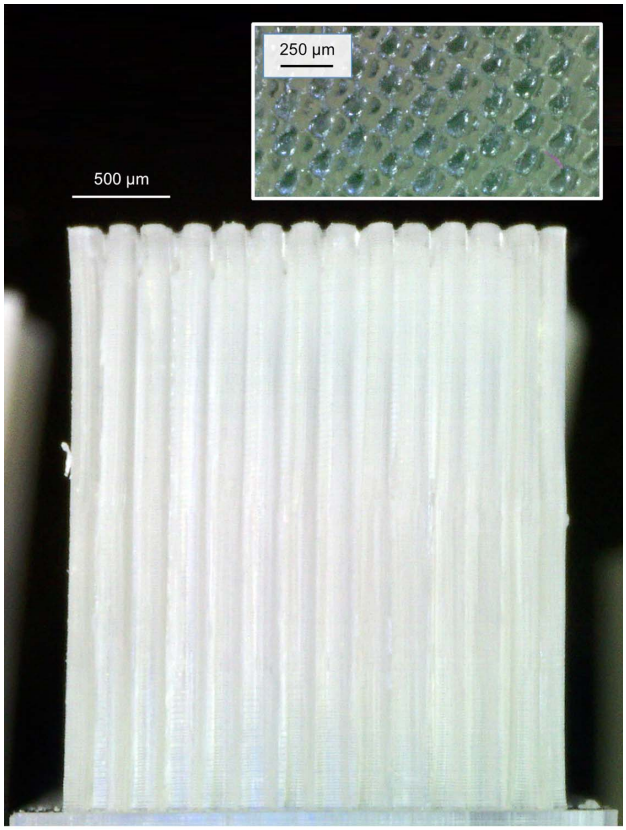

Fig. 4. Front view of an array of 3 mm tall, 179 $\pm$ 10 μm diameter solid columns with hexagonal packing and 200 μm $\pm$ 4 μm column pitch with close-up top view of a cluster of columns.

(i.e., the arrays of emitters are hexagonally packed with 700 $\pm$ 7 μm emitter pitch) were made; in these devices each emitter spout is fed by a 12 mm long internal channel with 377 $\pm$ 15 μm diameter (Figure 6).

IV. Device Characterization

A. Experimental Setup and Procedure

An schematic of the apparatus used to characterize the devices is shown in Figure 7. The electrospray array is clamped to an aluminum chuck using a set of polymer screws.

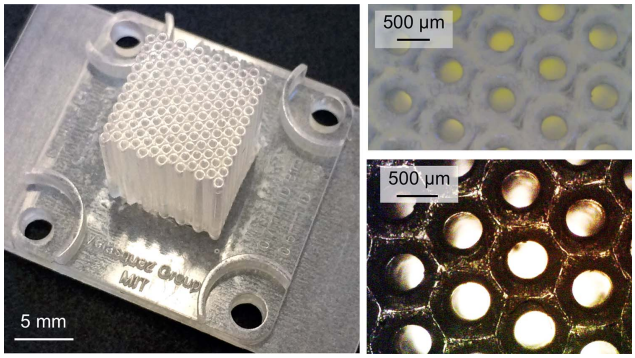

Fig. 5. A planar array of 143 tapered, internally fed electrospray emitters in 1 cm^2 (left) with close-up of the emitter spouts (top right) and the emitter inlets (bottom right). The emitters are fed by 12 mm long tapered internal channels with 400 $\pm$ 15 μm diameter at the emitter spout and 498 $\pm$ 10 μm diameter at the emitter inlet. In the picture of the emitter inlets, the edges of the smooth transitions that span the space between adjacent emitters is visible.

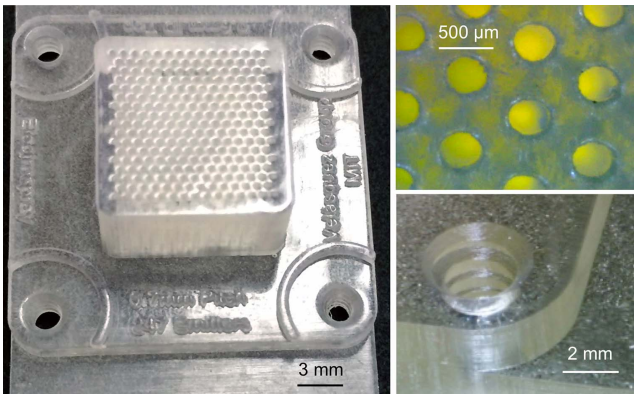

Fig. 6. A planar array of 236 internally fed electrospray emitters in 1 cm^2 (left) with close-up view of the emitter spouts (top right) and close-up view of a threaded hole (bottom right). The emitters are fed by 12 mm long straight internal channels with 377 $\pm$ 15 μm diameter.

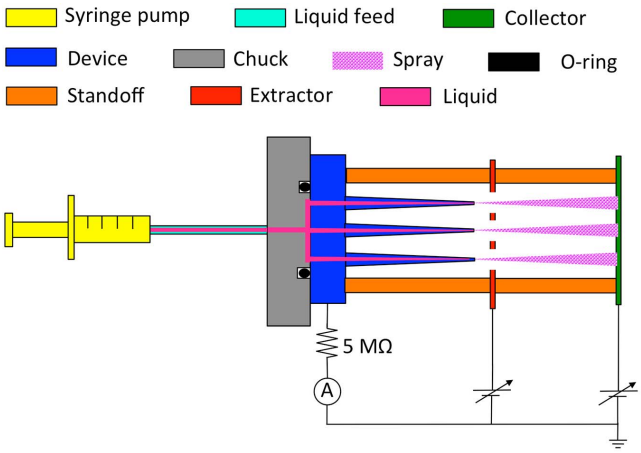

Fig. 7. Schematic of apparatus to electrically characterize the printed electrospray devices.

The chuck has a feedthrough that supplies liquid to the device, and an O-ring is used to seal the interface between the device and the chuck. The liquid is delivered to the chuck using a Harvard 33 syringe pump. The same screws that clamp the device to the chuck are used to integrate the extractor electrode, i.e., a laser-cut 250 μm-thick stainless

steel plate with apertures that line up with the emitters of the array, and the collector electrode, i.e., a 1/8"-thick aluminum plate. Ceramic spacers separate the electrospray array from the extractor electrode, and the extractor electrode from the collector electrode. The chuck is supported by four polymer legs that electrically isolate the chuck from the vibration isolation table that holds the apparatus. The chuck is connected to a Keithley 485 picoammeter through a high-voltage 5 MΩ resistor. The bias voltages applied to the extractor electrode and the collector electrodes are supplied by PC-controlled Gamma ES30P high voltage power supplies, each capable of delivering up to 30 kV and 200 μA in the positive polarity. The liquid utilized in the experiments was a mix of 1 mg/ml of Rhodamine B and 20 mg/ml of bovine serum albumin (BSA) solutions with a measured electrical conductivity equal to 1.3 Si/m. The Rhodamine B solution was made by diluting Rhodamine B powder supplied by Sigma-Aldrich (Sigma 83689) on StabilGuard Choice microarray stabilizer supplied by SurModics (SG02). The BSA solution was created by diluting BSA powder supplied by Sigma-Aldrich (Sigma A2153) on StabilGuard Choice microarray stabilizer supplied by SurModics (SG02). The mix of Rhodamine B and BSA solutions was filtered through a sterile 0.22 μm syringe filter. The Rhodamine B/BSA/StabilGuard Choice mixture was kept in storage at 6 °C in a refrigerator with a thermostat. A digital camera was used to monitor the chip. In a typical experiment, the electrospray array is first clamped to the chuck and the extractor and collector electrodes are integrated to the device, verifying that the extractor electrode and the emitter tips are well aligned. A syringe filled-in with liquid is installed in the syringe pump; the syringe is then connected to the liquid feed of the chuck and electrical connections to the chuck, extractor electrode, and collector electrode are made. The flow of liquid is started and the filling-in of the electrospray array is visually verified, including the formation of menisci on the emitter tips. The extractor and collector electrodes are then energized: the extractor electrode is biased at about 4.0 kV above the potential of the chuck to generate a single Taylor cone on each emitter, while the collector is biased at about 3 kV above the potential of the extractor electrode. After waiting for a few minutes the device operates steadily, and the currents are continuously recorded for several minutes. After this, the flow rate is increased, which triggers a transient until the emission is once more steady, and measurement of the currents is again conducted. After the experiments are completed, the direction of pumping is reversed to collect the liquid inside the apparatus; the electrodes are removed, the device is dismounted, and the parts in contact with the liquid are thoroughly cleaned with IPA using an ultrasonic bath, to then be dried with a nitrogen gun. Finally, the device is stored in a dry box and the syringe with liquid is stored in a refrigerator kept at 6 °C.

B. Experimental Results

The filling-in of the devices was characterized using a digital camera. It was observed that the channels fill-in at different rates; however, no dripping of liquid form the emitter spouts was seen during the array filling-in procedure of the devices with tapered channels (Figure 8), making possible to start the electrical operation of the device with a fully soaked device. The filling-in of devices with untapered channels using the same procedure resulted in liquid spilling before the full emitter array was soaked (Figure 9). Therefore, it is believed that the tapering of the channels facilitated the spill-free filling-in operation.

In each device tested, it was visually verified that all the emitters were filled-in and that each emitter was producing

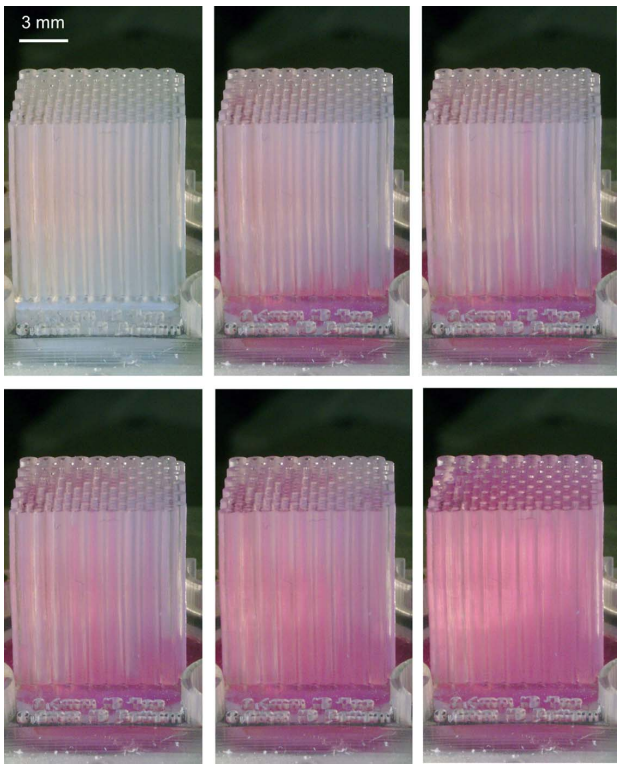

Fig. 8. Series of optical images that portray the filling-in of an array of 99 internally fed, tapered electrospray emitters (99 emitters in 1 cm^2). The procedure advances from left to right and from top to bottom.

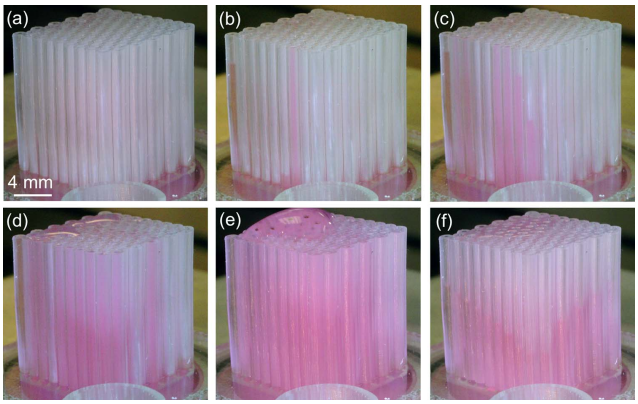

Fig. 9. (a) through (e): series of optical images that portray the filling-in of an array of 99 internally fed, untapered electrospray emitters (99 emitters in 1 cm^2); liquid dripping occurs before the device is fully soaked in liquid. (f) optical image of the device while the liquid is pulled back by reversing the direction of the flow, evidencing the cluster of emitters that flooded.

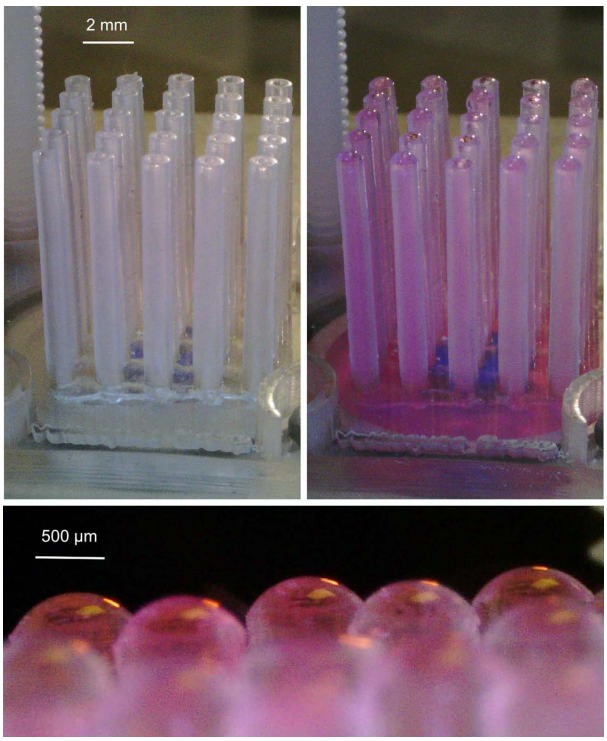

Fig. 10. An Array of 25 internally fed electrospray emitters dry (top left) and filled-in with liquid (top right). At the top of each emitter, a meniscus is formed (bottom).

a meniscus on its tip (Figure 10). The use of a translucent polymer to make the devices, and the use of a mixture containing Rhodamine B (a high-contrast red-colored dye) as working liquid greatly facilitated this operation.

Before conducing wet tests on each device characterized, the currents were measured with and without the operational voltages biased to the different electrodes of the apparatus while the device was still dry. The average current measured with the picoammeter while the bias voltages were on was equal to 5.1 $\pm$ 2.9 pA, which was very similar to the average current measured by the picoammeter without any bias voltages applied, i.e., 4.2 $\pm$ 1.6 pA. After running the device and flowing the liquid back into the syringe, the average current measured with the picoammeter while the bias voltages were on was visibly higher, i.e., 21.3 $\pm$ 3.9 pA, probably due to a thin coating of the dielectric posts caused by the operation of the device, but still orders of magnitude smaller than the currents measured during the operation of the electrospray sources. Therefore, it was concluded that the leakage current through the dielectric was very small and that the currents measured during the operation of the devices were caused by the electrospray.

Arrays of 1, 4, 9, 16, 25, and 49 electrospray emitters where characterized using per-emitter flow rates between 0.25 and 6.5 μl/min. An example of the Taylor cones generated during the experiments is shown in Figure 11. A log-log plot of per-emitter emitted current vs. per-emitter flow rate is shown in Figure 12. In this figure, it is assumed that the array is operating uniformly, that is, that the per-emitter current and flow rate are equal to dividing the total current and total flow rate by the number of emitters. The data fits well a power curve with exponent equal to 0.45, close to the square-root dependence reported for electrospray emitters that operate in the cone-jet mode [2]. As expected, the fluctuation of the per-emitter current is reduced with increasing emitter array size: for a single emitter, the average standard deviation is 9.6% of the average current, while for 4-emitter arrays the average standard deviation is reduced to 5.6% of the average current; for 9-emitter arrays the average standard deviation is reduced to 2.3% of the average current, whilst for 16-emitter arrays the average standard deviation is reduced to 1.1% of the average current; for 25-emitter arrays the average standard deviation is reduced to 0.8% of the average current, whereas for 49-emitter arrays the average standard deviation is reduced to 0.5% of the average current.

V. Discussion

Table 2 is a representative summary of the miniaturized, multiplexed, internally fed electrospray sources reported in the literature. The table includes the base material, minimum emitter pitch, maximum emitter density, and maximum array size reported in each case. The table does not include reported work on single-emitter sources (e.g., [37]–[39]), linear arrays of emitters (e.g., [17], [40]), planar arrays of emitters that are divided into individual emitters for assembly into an apparatus (e.g., [41]), or planar arrays that do not operate in parallel (e.g., [42], [43]); the table does not include either multiplexed miniaturized electrospray arrays with other kind of emitters (e.g., porous [14] or externally fed [15]). From Table 2 it can be realized that the SLA 3-D printed electrospray arrays reported in this work represent a twofold increase in emitter density and a sixfold increase in array size compared to the best values reported in the literature from miniaturized, multiplexed, polymer electrospray sources [24]. In addition, the 3-D printed devices have similar emitter density and larger array size compared to the majority of reported silicon MEMS multiplexed electrospray sources.

It is not surprising that there are reports of internally fed silicon MEMS multiplexed electrospray devices with visibly larger emitter density because the MFS of the photolithography used to make these devices is at least an order of magnitude smaller than the pixelation of the 3-D printer used in this work. However, in devices such as the one reported in [33], the emitter density is limited by the requirements of the rest of the system (e.g., the need of two proximal electrodes with high beam transmission), resulting in emitter densities on par with the results achieved using stereolithography. Therefore, there is an opportunity for satisfying applications using multiplexed polymer electrospray devices currently satisfied by silicon devices if the rest of the specifications besides the emitter density are met, e.g., temperature range and chemical compatibility.

One of the key reasons for using single-crystal silicon as building material in a large number of reported multiplexed electrospray sources is the correspondence between the dimensions of the emitters and the capabilities of DRIE. Silicon is also an excellent material of choice in applications associated with harsh conditions, e.g., combustors and nanosatellite

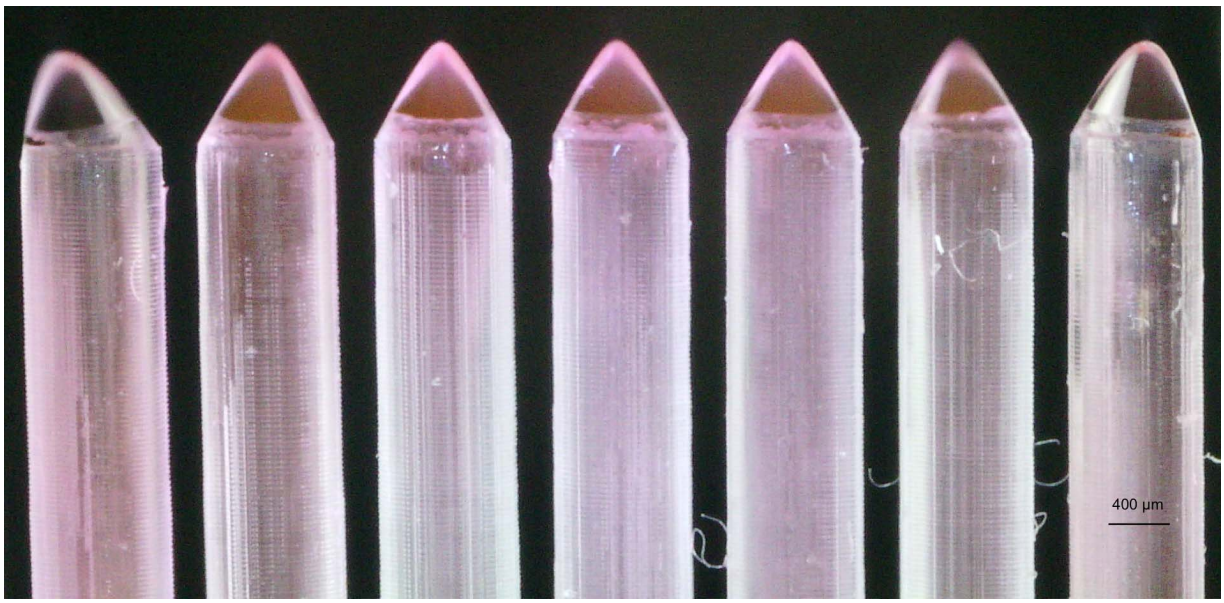

Fig. 11. External row of 7 emitters part of a 49-emitter array (emitter density 70 emitters/cm^2). The scalloping on the exterior of the emitters, due to the layer-by-layer manufacturing, is visible.

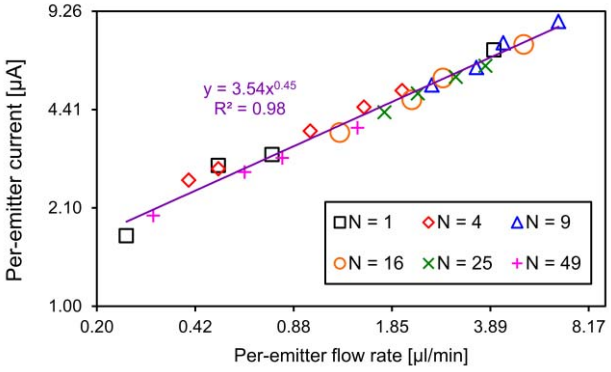

Fig. 12. Per-emitter current versus per-emitter flow rate for various arrays of electrospray emitters.

TABLE II
SUMMARY OF MINIATURIZED, MULTIPLEXED INTERNALLY FED ELECTROSPRAY EMITTER ARRAYS REPORTED IN THE LITERATURE. THE MAXIMUM ARRAY SIZE GIVEN IN THE TABLE IS AT THE MAXIMUM EMITTER DENSITY REPORTED

Ref.	Material	Min. E. pitch (µm)	Max. E. density (cm^{-2})	Max. A. Size
[11]	silicon	675	253 (hexagonal)	91
[13]	silicon	250	1,848 (hexagonal)	19
[33]	silicon	669	257 (hexagonal)	167
[34]	silicon	1,000	115 (hexagonal)	7
[35]	silicon	100	11,547 (hexagonal)	1,027
[24]	polymer	1,000	115 (hexagonal)	37
[36]	polymer	1,100	83 (square)	9
This work	polymer	700	236 (hexagonal)	236

electrical rockets. Nonetheless, polymer multiplexed electrospray sources would be advantageous in applications with less stringent conditions, e.g., low-temperature maskless micro and nanomanufacturing, water desalination [44], and mass spectrometry, because of the associated visibly lower cost per device and the visibly faster iteration turnaround of the design. The mass spectrometry application would also benefit from the disposable nature of the electrospray source given its visibly lower cost, this way avoiding cross-contamination of samples.

Besides the larger emitter density, the most important benefit from 3-D printing the electrospray devices compared to other fabrication approaches such as laser etching [36] or standard drilling [24] is the great versatility in the morphology of the source that can be implemented, including the fabrication of three-dimensional hydraulics (e.g., implementing for the first time monolithic arrays of microfabricated coaxial electrospray emitters [45]) and the monolithic integration of the electrospray source with the rest of the microfluidic system without added fabrication complexity.

Cell transfection, i.e., the process of deliberately introducing DNA into cells, is a very interesting potential application of the 3-D printed polymer electrospray arrays that cannot be satisfied with metal-based or semiconductor-based devices. Cell transfection is of tremendous importance because it is at the heart of the vaccine development process. State-of-the-art transfection is based on electroporation, where a momentary increase in the permeability of cell membrane occurs when the cells are exposed to short high-intensity electric field pulses. However, electroporation is time-consuming and has very low yield ($\sim 10^{-6}$). Ikemoto et al recently demonstrated that electrospray can be used to transfect cells with efficiencies as high as 93% if the emitter is made of a dielectric material instead of a metal or semiconductor [46]. Stereolithographic 3-D printed polymer electrospray arrays can be used to greatly increase the throughput of the already efficient electrospray-based transfection process, with the added advantage that the low cost of the 3-D printed part would make the transfection source disposable.

The range of electrospray device architectures that could be implemented using stereolithography would visibly increase if the manufacturing technology could be combined with other fabrication techniques. For example, internally fed emitters filled-in with microparticles could be made, analogous to what has been demonstrated in silicon MEMS multiplexed electrospray devices [13]. Also, externally fed devices with 3-D printed solid emitters coated with an engineered liquid wick could be implemented, analogous to the work reported on silicon MEMS/NEMS multiplexed sources [15], [28]; in this case, the wicking structure could be generated using a low-temperature process compatible with the printed polymer, e.g., hydrothermal synthesis of ZnO nanostructures [47]. In addition, lost-wax micromolded metal electrospray arrays can be made using stereolithographic 3-D printed wax masters; the emitters could be externally fed, or made porous through electrochemical etching similar to metal multiplexed electrospray devices reported in the literature [14].

An important pending issue is the ultimate capabilities of the SLA manufacturing technology, that is, how much denser the electrospray emitter arrays can be manufactured while still having low feature size variation across the array. There are other photosensitive polymers commercially available that have associated higher printing resolution and, in principle, one could also formulate to some degree the photosensitive resins used by the tool; in addition, the length of the channels could be reduced, which should make feasible printing devices with significantly smaller MFS and larger emitter array density. In these devices, active alignment of the electrode grids, e.g., using clusters of miniaturized deflection springs [48], [49], might be required to achieve high spray transmission. However, it is not expected a dramatic improvement in the MFS and emitter array density by optimizing the photosensitive polymer and device morphology because the resolution of the 3-D printer is limited by the XY pixelation, which is set by the size and pitch of the laser diodes, added to the fact that, in general, a plurality of pixels are required to accurately resolve a general shape [50]. However, it might be possible to substantially decrease the MFS without changing the 3-D printer, modifying the printing recipe, or sacrificing the feature uniformity across the array if a uniform conformal coating is applied to the printed part. For example, deposition of parylene C, a poly(p-xylylene) polymer, could be an interesting possibility to explore given parylene's low-temperature and low-vacuum deposition conditions, as well as its high deposition uniformity and excellent breakdown voltage; other researchers have already demonstrated polydimethylsiloxane (PDMS) microfluidics coated with parylene [51] and parylene electrospray ionizers [52]. Stereolithography is ultimately limited by the wavelength of the light used to expose the photosensitive polymer, which is in the near-ultraviolet range. There are commercial stereolithographic 3-D printers with demonstrated capability for making mesoscaled parts with submicron resolution [27] that could be used to print multiplexed electrospray arrays and other microfluidics with the same MFS, emitter array density, and emitter array size already demonstrated in silicon. These tools are fairly expensive at this moment, which puts them at odds with the original motivation to demonstrate low-cost manufacturing of multiplexed electrospray sources to extend their application beyond high-end applications and research; however it is expected that as SLA hardware improves and becomes less expensive, the limitation in the XY pixelation will relax.

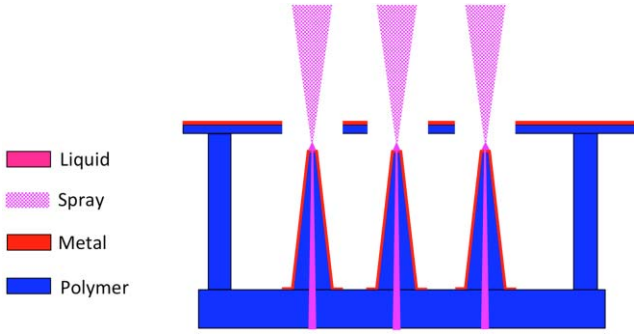

Fig. 13. A schematic cross section of a 3-D printed electrospray emitter array with monolithically integrated extractor grid.

Finally, a possible improvement in the fabrication of the electrospray devices would be the monolithic integration of electrodes with apertures aligned to the emitter array. The devices tested in this work used laser-cut grids as extractor electrode. Even though devices with as many as 236 emitters in 1 cm^2 were made, extractor electrodes with over 49 emitters in 1 cm^2 were not manufactured due to the limitations of the laser tool used to etch the grids; it is also possible that problems with alignment and beam interception could surface for arrays of high emitter density due to the length of the emitters and the assembly approach. A plausible idea to achieve the monolithic integration of the extractor to the emitter array is the use of directional deposition, e.g., electron beam evaporation of a metallic film, as shown in Figure 13. In this approach, the printed part has features out of the line of sight of the directional deposition to avoid shorting the electrode grid. The demonstration of this idea would require some groundwork, including the characterization of the printed polymer as a high-voltage electrical insulator, and the investigation of the interaction of the printed part with the deposited film(s) in aspects such as surface adhesion, thermal damage of the surface, and thermal deformation of the part. A possibility to minimize the thermal effects caused by the metal deposition is to evaporate a very thin seed layer and then complete the deposition of the metal layer via electroless plating, which has been shown to work well with dielectric substrates [53].

VI. Conclusion

The design, fabrication, and characterization of miniaturized arrays of polymer electrospray emitters fabricated with stereolithography has been reported. The additive manufacturing technique allows great freedom in the device architecture and has associated two orders of magnitude reduction in the production cost per device, infrastructure cost, and the fabrication time compared to a silicon MEMS multiplexed electrospray source. Through optimization of the fabrication process, arrays with as many as 236 internally fed electrospray emitters in 1 cm^2 were made, i.e., a sixfold increase in array

size and a twofold increase in emitter density compared to the best reported values from multiplexed, internally fed polymer electrospray sources [24]. Characterization of devices with different array size demonstrated uniform emitter operation. Tentative applications of the technology include low-temperature maskless micro/nanomanufacturing, water desalination, and mass spectrometry.

ACKNOWLEDGEMENTS

The devices were fabricated at the Microsystems Technology Laboratories of the Massachusetts Institute of Technology. The author would like to thank Tyler Teague from JETT Research & Proto Products (Fairview, TN) for useful conversations on SLA 3-D printing, and Patrick Marek from the US Army Natick Soldier Research Development and Engineering Center (Natick, MA) for supplying the solution of Rhodamine B, bovine serum albumin and StabilGuard Choice microarray stabilizer that was used in the experiments.

REFERENCES

[1] G. Taylor, "Disintegration of water drops in an electric field," *Proc. R. Soc. Lond. A, Math. Phys. Sci.*, vol. 280, no. 1382, pp. 383–397, 1964.

[2] J. F. de la Mora and I. G. Loscertales, "The current emitted by highly conducting Taylor cones," *J. Fluid Mech.*, vol. 260, pp. 155–184, Feb. 1994.

[3] I. Romero-Sanz, R. Bocanegra, J. F. de la Mora, and M. Gamero-Castaño, "Source of heavy molecular ions based on Taylor cones of ionic liquids operating in the pure ion evaporation regime," *J. Appl. Phys.*, vol. 94, no. 4, pp. 3599–3605, 2003.

[4] J. Doshi and D. H. Reneker, "Electrospinning process and applications of electrospun fibers," *J. Electrostatics*, vol. 35, nos. 2–3, pp. 151–160, Aug. 1995.

[5] C. M. Waits, B. Hanrahan, and I. Lee, "Multiplexed electrospray scaling for liquid fuel injection," *J. Micromech. Microeng.*, vol. 20, no. 10, pp. 104010-1–104010-10, 2010.

[6] A. Jaworek, "Electrospray droplet sources for thin film deposition," *J. Mater. Sci.*, vol. 42, no. 1, pp. 266–297, 2007.

[7] M. Gamero-Castaño and V. Hruby, "Electrospray as a source of nanoparticles for efficient colloid thrusters," *J. Propuls. Power*, vol. 17, no. 5, pp. 977–987, 2001.

[8] J. B. Fenn, M. Mann, C. K. Meng, S. F. Wong, and C. M. Whitehouse, "Electrospray ionization for mass spectrometry of large biomolecules," *Science*, vol. 246, no. 4926, pp. 64–71, 1989.

[9] Y.-X. Wang, J. W. Cooper, C. S. Lee, and D. L. DeVoe, "Efficient electrospray ionization from polymer microchannels using integrated hydrophobic membranes," *Lab. Chip*, vol. 4, no. 4, pp. 363–367, 2004.

[10] L. F. Velásquez-García, A. I. Akinwande, and M. Martínez-Sánchez, "A planar array of micro-fabricated electrospray emitters for thruster applications," *J. Microelectromech. Syst.*, vol. 15, no. 5, pp. 1272–1280, Oct. 2006.

[11] W. Deng, J. F. Klemic, X. Li, M. A. Reed, and A. Gomez, "Increase of electrospray throughput using multiplexed microfabricated sources for the scalable generation of monodisperse droplets," *J. Aerosol Sci.*, vol. 37, no. 6, pp. 696–714, Jun. 2006.

[12] B. Gassend, L. F. Velásquez-García, A. I. Akinwande, and M. Martinez-Sanchez, "A microfabricated planar electrospray array ionic liquid ion source with integrated extractor," *J. Microelectromech. Syst.*, vol. 18, no. 3, pp. 679–694, Jun. 2009.

[13] R. Krpoun and H. R. Shea, "Integrated out-of-plane nanoelectrospray thruster arrays for spacecraft propulsion," *J. Micromech. Microeng.*, vol. 19, no. 4, p. 045019, 2009.

[14] H. Q. Li, D. G. Courtney, P. D. G. Maqueo, and P. Lozano, "Fabrication and testing of an ionic electrospray propulsion system with a porous metal tip array," in *Proc. 16th IEEE Int. Conf. Solid-State Sens., Actuators, Microsyst.*, Beijing, China, Jun. 2011, pp. 1998–2001.

[15] F. A. Hill, E. V. Heubel, P. P. de Leon, and L. F. Velásquez-García, "High-throughput ionic liquid ion sources using arrays of microfabricated electrospray emitters with integrated extractor grid and carbon nanotube flow control structures," *J. Microelectromech. Syst.*, vol. 23, no. 5, pp. 1237–1248, Oct. 2014.

[16] B. L. P. Gassend, L. F. Velásquez-García, and A. I. Akinwande, "Design and fabrication of DRIE-patterned complex needlelike silicon structures," *J. Microelectromech. Syst.*, vol. 19, no. 3, pp. 589–598, Jun. 2010.

[17] L. F. Velásquez-García, A. I. Akinwande, and M. Martínez-Sánchez, "A micro-fabricated linear array of electrospray emitters for thruster applications," *J. Microelectromech. Syst.*, vol. 15, no. 5, pp. 1260–1271, Oct. 2006.

[18] K. V. Wong and A. Hernandez, "A review of additive manufacturing," *ISRN Mech. Eng.*, vol. 2012, pp. 208760-1–208760-10, Jun. 2012.

[19] M. Vaezi, H. Seitz, and S. Yang, "A review on 3D micro-additive manufacturing technologies," *Int. J. Adv. Manuf. Technol.*, vol. 67, nos. 5–8, pp. 1721–1754, Jul. 2013.

[20] R. T. Chen, E. R. Brown, and R. S. Singh, "A compact 30 GHz low loss balanced hybrid coupler fabricated using micromachined integrated coax," in *Proc. IEEE Radio Wireless Conf.*, Atlanta, GA, USA, Sep. 2004, pp. 227–230.

[21] P. Johander, S. Haasl, K. Persson, and U. Harrysson, "Layer manufacturing as a generic tool for microsystem integration,"in *Proc. Conf. Multi-Material Micro Manuf. (4M)*, Borovets, Bulgaria, Oct. 2007.

[22] J. J. Adams *et al.*, "Conformal printing of electrically small antennas on three-dimensional surfaces," *Adv. Mater.*, vol. 23, no. 11, pp. 1335–1340, Mar. 2011.

[23] R. Krpoun, K. L. Smith, J. P. W. Stark, and H. R. Shea, "Tailoring the hydraulic impedance of out-of-plane micromachined electrospray sources with integrated electrodes," *Appl. Phys. Lett.*, vol. 94, no. 16, pp. 163502-1–163502-3, 2009.

[24] R. Bocanegra, D. Galán, M. Márquez, I. G. Loscertales, and A. Barrero, "Multiple electrosprays emitted from an array of holes," *J. Aerosol Sci.*, vol. 36, no. 12, pp. 1387–1399, Dec. 2005.

[25] J. M. L. Urdiales, "Progress in colloid propulsion," M.S. thesis, Dept. Aeronautics Astron., Massachusetts Institute of Technology, Cambridge, MA, USA, Sep. 2004.

[26] P. D. Prewett and G. L. R. Mair, *Focused Ion Beams From Liquid Metal Ion Sources*. Hertfordshire, U.K.: Research Studies Press, 1991.

[27] [Online]. Available: http://www.nanoscribe.de/files/8414/3798/6567/DataSheet_Photonic_Professional_GT.pdf, accessed Sep. 3, 2015.

[28] P. J. P. de Leon, F. A. Hill, E. V. Heubel, and L. F. Velásquez-García, "Parallel nanomanufacturing via electrohydrodynamic jetting from microfabricated externally fed emitter arrays," *Nanotechnology*, vol. 26, no. 22, pp. 225301-1–225301-10, 2015.

[29] *Asiga Pico Plus 27*. [Online]. Available: https://www.asiga.com/media/main/files/Pico%20Brochure_us_en.pdf, accessed Sep. 3, 2015.

[30] F. P. W. Melchels, J. Feijen, and D. W. Grijpma, "A review on stereolithography and its applications in biomedical engineering," *Biomaterials*, vol. 31, no. 24, pp. 6121–6130, Aug. 2010.

[31] [Online]. Available: https://www.asiga.com/media/main/files/PlasCLEAR_us_en.pdf, accessed Sep. 3, 2015.

[32] K.-S. Chen, A. Ayon, and S. M. Spearing, "Controlling and testing the fracture strength of silicon on the mesoscale," *J. Amer. Ceram. Soc.*, vol. 83, no. 6, pp. 1476–1484, Jun. 2000.

[33] S. Dandavino *et al.*, "Microfabricated electrospray emitter arrays with integrated extractor and accelerator electrodes for the propulsion of small spacecraft," *J. Micromech. Microeng.*, vol. 24, no. 7, pp. 075011-1–075011-13, 2014.

[34] G. Lenguito and A. Gomez, "Pressure-driven operation of microfabricated multiplexed electrosprays of ionic liquid solutions for space propulsion applications," *J. Microelectromech. Syst.*, vol. 23, no. 3, pp. 689–698, Jun. 2014.

[35] W. Deng, C. M. Waits, B. Morgan, and A. Gomez, "Compact multiplexing of monodisperse electrosprays," *J. Aerosol Sci.*, vol. 40, no. 10, pp. 907–918, Oct. 2009.

[36] K. Tang, Y. Lin, D. W. Matson, T. Kim, and R. D. Smith, "Generation of multiple electrosprays using microfabricated emitter arrays for improved mass spectrometric sensitivity," *Anal. Chem.*, vol. 73, no. 8, pp. 1658–1663, 2001.

[37] R. S. Ramsey and J. M. Ramsey, "Generating electrospray from microchip devices using electroosmotic pumping," *Anal. Chem.*, vol. 69, no. 6, pp. 1174–1178, 1997.

[38] A. Desai, Y.-C. Tai, M. T. Davis, and T. D. Lee, "A MEMS electrospray nozzle for mass spectroscopy," in *Proc. Transducers*, Chicago, IL, USA, Jun. 1997, pp. 927–930.

[39] A. K. Sen, J. Darabi, and D. R. Knapp, "Design, fabrication and test of a microfluidic nebulizer chip for desorption electrospray ionization mass spectrometry," *Sens. Actuators B, Chem.*, vol. 137, no. 2, pp. 789–796, Apr. 2009.

[40] W. Kim, M. Guo, P. Yang, and D. Wang, "Microfabricated monolithic multinozzle emitters for nanoelectrospray mass spectrometry," *Anal. Chem.*, vol. 79, no. 10, pp. 3703–3707, 2007.
[41] P. Griss, J. Melin, J. Sjödahl, J. Roeraade, and G. Stemme, "Development of micromachined hollow tips for protein analysis based on nanoelectrospray ionization mass spectrometry," *J. Micromech. Microeng.*, vol. 12, no. 5, pp. 682–687, 2002.
[42] G. A. Schultz, T. N. Corso, S. J. Prosser, and S. Zhang, "A fully integrated monolithic microchip electrospray device for mass spectrometry," *Anal. Chem.*, vol. 72, no. 17, pp. 4058–4063, 2000.
[43] C.-H. Yuan and J. Shiea, "Sequential electrospray analysis using sharp-tip channels fabricated on a plastic chip," *Anal. Chem.*, vol. 73, no. 6, pp. 1080–1083, 2001.
[44] S. P. Brouwer, "Design and characterization of a single-effect electrohydrodynamic desalinator," M.S. thesis, Dept. Mech. Eng., Delft Univ. Technol., Delft, The Netherlands, 2011.
[45] I. G. Loscertales, A. Barrero, I. Guerrero, R. Cortijo, M. Marquez, and A. M. Gañán-Calvo, "Micro/nano encapsulation via electrified coaxial liquid jets," *Science*, vol. 295, no. 5560, pp. 1695–1698, Mar. 2002.
[46] K. Ikemoto, I. Sakata, and T. Sakai, "Collision of millimetre droplets induces DNA and protein transfection into cells," *Sci. Rep.*, vol. 2, pp. 289–294, Feb. 2012.
[47] S. Baruah and J. Dutta, "Hydrothermal growth of ZnO nanostructures," *Sci. Technol. Adv. Mater.*, vol. 10, no. 1, pp. 013001-1–013001-18, 2009.
[48] L. F. Velásquez-García, A. I. Akinwande, and M. Martínez-Sánchez, "Precision hand assembly of MEMS subsystems using DRIE-patterned deflection spring structures: An example of an out-of-plane substrate assembly," *J. Microelectromech. Syst.*, vol. 16, no. 3, pp. 598–612, Jun. 2007.
[49] B. Gassend, L. F. Velásquez-García, and A. I. Akinwande, "Precision in-plane hand assembly of bulk-microfabricated components for high-voltage MEMS arrays applications," *J. Microelectromech. Syst.*, vol. 18, no. 2, pp. 332–346, Apr. 2009.
[50] T. Acharya and A. K. Ray, *Image Processing: Principles and Applications*. Hoboken, NJ, USA: Wiley, 2005.
[51] Y. S. Shin *et al.*, "PDMS-based micro PCR chip with parylene coating," *J. Micromech. Microeng.*, vol. 13, no. 5, pp. 768–774, 2003.
[52] T. Sikanen, S. Franssila, T. J. Kauppila, R. Kostiainen, T. Kotiaho, and R. A. Ketola, "Microchip technology in mass spectrometry," *Mass Spectrometry Rev.*, vol. 29, no. 3, pp. 351–391, May/Jun. 2010.
[53] K. Cheng *et al.*, "Ink-jet printing, self-assembled polyelectrolytes, and electroless plating: Low cost fabrication of circuits on a flexible substrate at room temperature," *Macromolecular Rapid Commun.*, vol. 26, no. 4, pp. 247–264, Feb. 2005.

Luis Fernando Velásquez-García (M'09–SM'10) received the Mechanical Engineer and Civil Engineer degrees (magna cum laude and valedictorian of the School of Engineering in both cases) from the Universidad de Los Andes, Bogotá, Colombia, in 1998 and 1999, respectively, and the M.S. and Ph.D. degrees from the Department of Aeronautics and Astronautics, Massachusetts Institute of Technology (MIT), Cambridge, MA, USA, in 2001 and 2004, respectively.

He became a Post-Doctoral Associate with Microsystems Technology Laboratories, MIT, in 2004, after completing his studies, where he was appointed as a Research Scientist in 2005. Since 2009, he has been a Principal Scientist and Core Member with Microsystems Technology Laboratories. He is an Expert in micro and nanofabrication technologies, and his research focuses on micro and nanoenabled multiplexed scaled-down systems for space, energy, healthcare, manufacturing, and analytical applications that exploit high-electric field phenomena, e.g., electrospray, electrospinning, electron impact ionization, field ionization, field emission, X-rays, and plasmas. He has authored over 35 journal publications and 55 conference proceedings publications, and he holds 15 patents on MEMS/NEMS technologies. He currently serves as the Co-Chair of the 15th International Workshop on Micro and Nanotechnology for Power Generation and Energy Conversion Applications (PowerMEMS 2015).

Dr. Velásquez-García is a Full Member of Sigma Xi and a Senior Member of the American Institute of Aeronautics and Astronautics.